Organic & Biomolecular Chemistry

Cite this: *Org. Biomol. Chem.*, 2012, **10**, 3258

www.rsc.org/obc

PAPER

Solid-phase-assisted synthesis of targeting peptide–PEG–oligo(ethane amino) amides for receptor-mediated gene delivery†

Irene Martin,[a] Christian Dohmen,[b] Carlos Mas-Moruno,[c,d] Christina Troiber,[b] Petra Kos,[b] David Schaffert,[b] Ulrich Lächelt,[b] Meritxell Teixidó,[a] Michael Günther,[b] Horst Kessler,[c,d] Ernest Giralt*[a] and Ernst Wagner*[b]

Received 11th November 2011, Accepted 23rd February 2012
DOI: 10.1039/c2ob06907e

In the forthcoming era of cancer gene therapy, efforts will be devoted to the development of new efficient and non-toxic gene delivery vectors. In this regard, the use of Fmoc/Boc-protected oligo(ethane amino) acids as building blocks for solid-phase-supported assembly represents a novel promising approach towards fully controlled syntheses of effective gene vectors. Here we report on the synthesis of defined polymers containing the following: (i) a plasmid DNA (pDNA) binding domain of eight succinoyl-tetraethylenpentamine (Stp) units and two terminal cysteine residues; (ii) a central polyethylene glycol (PEG) chain (with twenty-four oxyethylene units) for shielding; and (iii) specific peptides for targeting towards cancer cells. Peptides B6 and c(RGDfK), which bind transferrin receptor and $\alpha_v\beta_3$ integrin, respectively, were chosen because of the high expression of these receptors in many tumoral cells. This study shows the feasibility of designing these kinds of fully controlled vectors and their success for targeted pDNA-based gene transfer.

Introduction

Cancer is one of the most aggressive diseases known, and surgery and conventional chemotherapy often do not provide satisfactory therapeutic benefit. In the case of metastasis, tumor-targeted gene therapies would be highly desirable to introduce lethal genes into tumors, thereby inducing apoptosis or immune responses or blocking neoangiogenesis. Receptor-targeted synthetic gene delivery methods[1–4] appear to be a promising solution; however, their chemistry and biological efficiency require further improvement.

Many kinds of polymers for the delivery of nucleic acids into cells have been developed since 1962 (first application: delivery of infectious poliovirus RNA).[5–7] Receptor-mediated DNA delivery by targeting polymer conjugates was first introduced by Wu and Wu in 1987.[8] Asialoglycoprotein–polylysine conjugates were used for the formation of so-called polyplexes[9] by the electrostatic interaction of a negatively charged plasmid DNA (pDNA) and the polycationic polymer. In this form, pDNA was protected from degradation in the blood and targeted for *in vivo* expression in hepatocytes. Nevertheless, polyplex uptake into the cells by the endocytic pathway poses a significant problem: entrapment in the endolysosomal compartment strongly limits the efficiency of polyplexes. Endosomal release was ameliorated by introduction of lysosomotropic agents such as chloroquine,[10] endosomolytic peptides,[10,11] or with polymers such as polyethylenimine (PEI)[12] with inherent endosomal-escape properties.

The "proton sponge" effect[13–16] of PEI, namely the buffering capacity between neutral and endosomal pH contributes to the destabilization of endosomes and release of polyplexes into the cytosol. Thus, PEI is one of the most advantageous, commonly used cationic transfection polymers. However, there are several aspects where further optimization of PEI-like polymers can be considered. Improved biocompatibility of PEI would be beneficial; PEI of various molecular weights and structures may induce membrane damage when present at higher concentrations, thus causing cell death by apoptosis.[17,18] Also interactions with blood cells[19] and activation of the complement system[20] decrease biocompatibility, efficiency, and target specificity. In this regard, effort has been made to reduce the toxicity of PEI

[a]*Institute for Research in Biomedicine (IRB Barcelona), Barcelona Science Park (PCB), Baldiri Reixac 10, 08028 Barcelona, Spain. E-mail: ernest.giralt@irbbarcelona.org; Fax: (+34) 93-4037126*
[b]*Pharmaceutical Biotechnology, Center for Nanoscience, Ludwig-Maximilians-University Munich, Butenandtstrasse 5-13, 81377 Munich, Germany. E-mail: ernst.wagner@cup.uni-muenchen.de; Fax: (+49) 89 2180 77891*
[c]*Institute for Advanced Study and Center of Integrated Protein Science, Department of Chemistry, TU Munich, Lichtenbergstr. 4, 85747 Garching, Germany*
[d]*Faculty of Science, King Abdulaziz University, P.O. Box 80203, 21589 Jeddah, Saudi Arabia*

†Electronic supplementary information (ESI) available. Figures S1–S4. NMR spectra. Figure S5. RP-HPLC profiles. Figure S6. Mass spectrometry data. Figure S7. Size and zeta potential data from dynamic light scattering (DLS). Figure S8. TEM images of Ala-K ((C-Stp4)2-K-A) polyplex. Figures S9-S12. MTT assays. Figure S13. Transferrin competition assays in N2A and DU-145 cells. Figure S14. Cilengitide competition assays in Du-145 cells. Figures S15. Erythrocyte lysis assay of the polymers at a range of pH values. See DOI: 10.1039/c2ob06907e

without decreasing its benefits in gene transfer. As toxicity is correlated with polymer size, biodegradable PEI analogs that degrade into non-toxic smaller fragments have been developed.[21–23] Other strategies focus on targeting moieties and surface shielding of polyplexes using polyethylene glycol (PEG) bound to PEI,[24,25] in some cases by pH-sensitive linkers.[26,27] Like many other conventional polymers, another limitation of PEI is the inherent polydispersity in molecular weight and the heterogeneity of modification sites in chemical conjugates. One solution to overcome this limitation would be the use of solid-phase peptide synthesis (SPPS) methodologies, but using defined oligoamine building blocks instead of amino acids. In this regard Hartmann and colleagues[28–30] generated precise, sequence-defined cationic polymers for pDNA polyplex formation. We adapted this strategy by designing novel Fmoc/Boc-protected oligo(ethane amino)acids as building blocks.[31] These blocks are fully compatible with SPPS conditions and contain oligoethylenimine motifs, which are considered responsible for the high efficiency of PEI. In a proof of concept study, we synthesized a polymer library of highly pure monodisperse polymers with full control of their chemical composition and structure.[32] Several polymer candidates showed high transfection efficacy for DNA and siRNA delivery and low toxicity.[32]

Here we provide the first description of the synthesis of precise peptide–PEG–oligo(ethane amino)amide polymers and their successful use in receptor-targeted, surface-shielded pDNA polyplexes. We tested two examples of tumor-targeting peptides which specifically recognize receptors that are highly expressed in tumor cells. These peptides were B6 peptide (GHKAKGPRK), which binds to the transferrin receptor,[33] and c(RGDfK), which binds with high affinity and selectivity to $\alpha_v\beta_3$ integrin.[34–36] Targeting peptides were attached at one end of a monodisperse PEG molecule as shielding moiety. The oligo(ethane amino)amide polycation for pDNA binding and condensation was linked in a T-shape configuration to the other end of the PEG chain (Fig. 1). Terminal cysteine residues were included for polyplex stabilization by disulfide bond formation. The polymeric constructs were synthesized on solid phase and their efficacy in receptor-specific pDNA transfer was successfully demonstrated in two tumor cell lines.

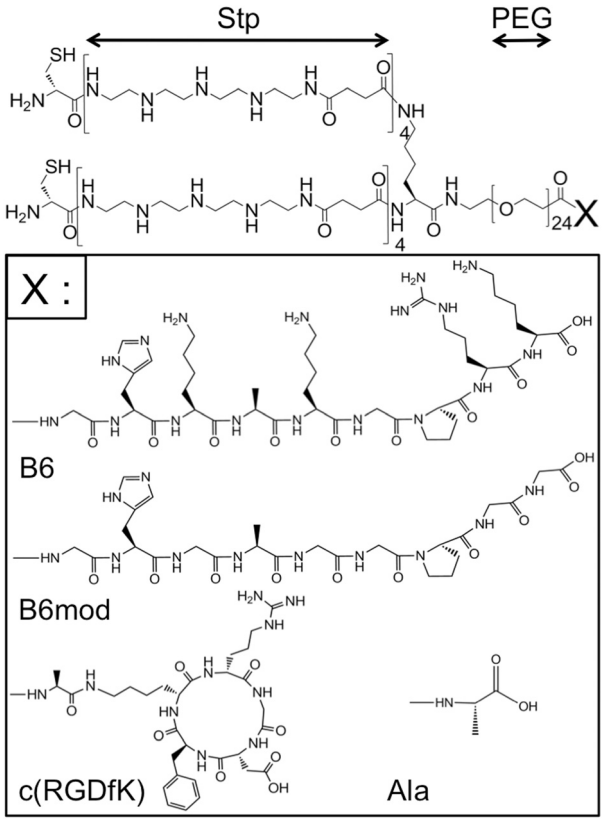

Fig. 1 Chemical structure of polymers prepared. Stp = succinoyl-tetraethylenpentamine units; PEG = polyethylene glycol units; X = peptide motif: B6, transferrin-receptor targeting polymer $(C\text{-}Stp_4)_2$-K-PEG-B6; B6mod, transferrin-receptor targeting negative control polymer $(C\text{-}Stp_4)_2$-K-PEG-B6mod; c(RGDfK), $\alpha_v\beta_3$-targeting polymer $(C\text{-}Stp_4)_2$-K-PEG-A-cRGDfK; Ala, negative control polymer $(C\text{-}Stp_4)_2$-K-PEG-A.

Results and discussion

Peptide and polymer synthesis

The objective of this study was to design targeted polymers for pDNA delivery following a fully controlled and precise synthetic methodology, and to evaluate the biological profile of these structures in cell culture as a first approach for targeting DNA delivery *in vivo*. For this purpose, we designed four polymers that share the same polymeric scaffold but present distinct targeting peptides (Fig. 1). These molecules consist (from C- to N-terminus) of a targeting or negative control peptide, a precise PEG moiety for shielding that contains 24 oxyethylene units, a branching unit (lysine) extended by the nucleic acid binding domain with four succinoyl-tetraethylenpentamine (Stp) units,[31] and terminal cysteine residues at the end of the two Stp_4 arms. The Stp units refer to the novel oligo(ethane amino)amide building blocks for pDNA binding.[31] These Stp units were added sequentially in their Fmoc/Boc-protected form to the growing polymer chain using conventional SPPS protocols. Concerning the targeting sequences, two bioactive epitopes were chosen (Fig. 1, structures B6 and c(RGDfK)). The B6 peptide[33] (GHKAKGPRK) targets the human transferrin receptor (hTfR), which is overexpressed in various cancers, and has already been successfully applied in targeted polyplexes.[37–39] RGD is a well-known recognition motif that binds to integrins,[40,41] and these receptors are overexpressed in many tumor cell types and tumor vasculature.[42] The cyclic RGD peptide c(RGDfK)[34,36] shows high affinity and selectivity for $\alpha_v\beta_3$ integrin.[43] Both integrins[25,44–49] and TfR[49–53] have been successfully evaluated as suitable targets for nucleic acid delivery to cancer cells. As inactive controls, we used either a modified peptide derived from B6 (B6mod, where lysine and arginine residues are replaced by glycine, GHGAGGPGG) or, instead of the cyclic RGD peptide, the simple amino acid residue alanine (Fig. 1, structures B6mod and Ala).

B6, B6mod and Ala polymers ($(C\text{-}Stp_4)_2$-K-PEG-B6, $(C\text{-}Stp_4)_2$-PEG-B6mod and $(C\text{-}Stp_4)_2$-PEG-A, respectively) were assembled stepwise on solid-phase. Alternatively, the c(RGDfK) polymer ($(C\text{-}Stp_4)_2$-K-PEG-A-c(RGDfK)) was obtained *via* coupling in solution of the conveniently protected cyclic RGD peptide and the polymeric scaffold, both previously prepared

using SPPS (see Materials and methods section for further details). Each polymer was characterized by ^{1}H-NMR, RP-HPLC and mass spectrometry (Fig. S1–S6, ESI†).

Polyplex characterization

Having synthesized and characterized the polymers, we studied the characteristics of their interaction with the pDNA in order to gain a better knowledge of the nature of these new gene delivery vectors. Polyplexes were formed at a range of polymer/pDNA ratios defined by protonable nitrogen/phosphate molar ratios (N/P ratios), using fixed amounts of pDNA (pCMVeGFPLuc, 200 ng). The agarose gel shift assay displayed in Fig. 2 shows the pDNA binding capacity of the B6, c(RGDfK), B6mod and Ala polymers at the N/P ratios tested. All the polymers retained pDNA at a N/P ratio of 20, thereby indicating satisfactory pDNA binding, which is essential for their transfection efficacy. B6 polymer retains pDNA better than the other polymers, probably due to the presence of positively charged residues in its sequence. This issue will be further discussed in the following sections. The particle size and structure of the polyplexes were analyzed by transmission electron microscopy (TEM) (Fig. 3), atomic force microscopy (AFM) (Fig. 4) and dynamic light scattering (DLS) (Fig. S7, ESI†). Polyplexes at a N/P ratio of 20 adopted a "doughnut" shape measuring around 70–100 nm in

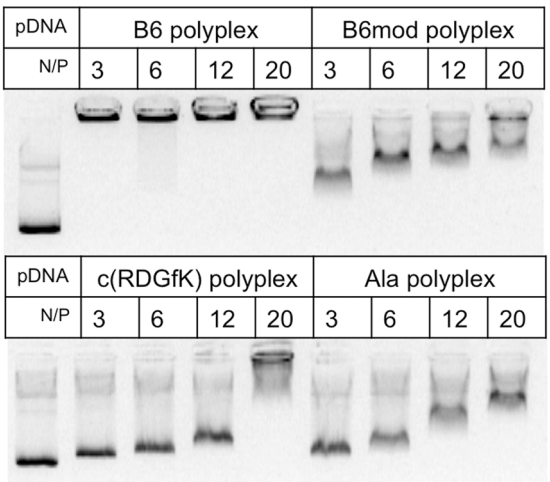

Fig. 2 pDNA binding capacity of B6, B6mod, c(RGDfK) and Ala polymers as determined by means of an agarose gel shift assay at a range of N/P ratios (3 : 1, 6 : 1, 12 : 1 and 20 : 1). pDNA polyplex formation was performed following transfection conditions (30 min of incubation in HEPES-buffered glucose (HBG)).

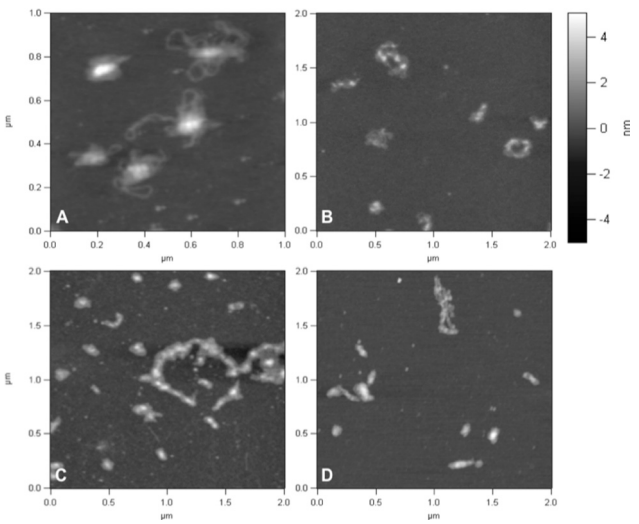

Fig. 4 AFM images of polyplexes (N/P ratio of 20 : 1) placed on a mica surface and dried RT for 5–10 min. (A) B6 polyplex; (B) B6mod polyplex; (C) c(RGDfK) polyplex; (D) Ala polyplex.

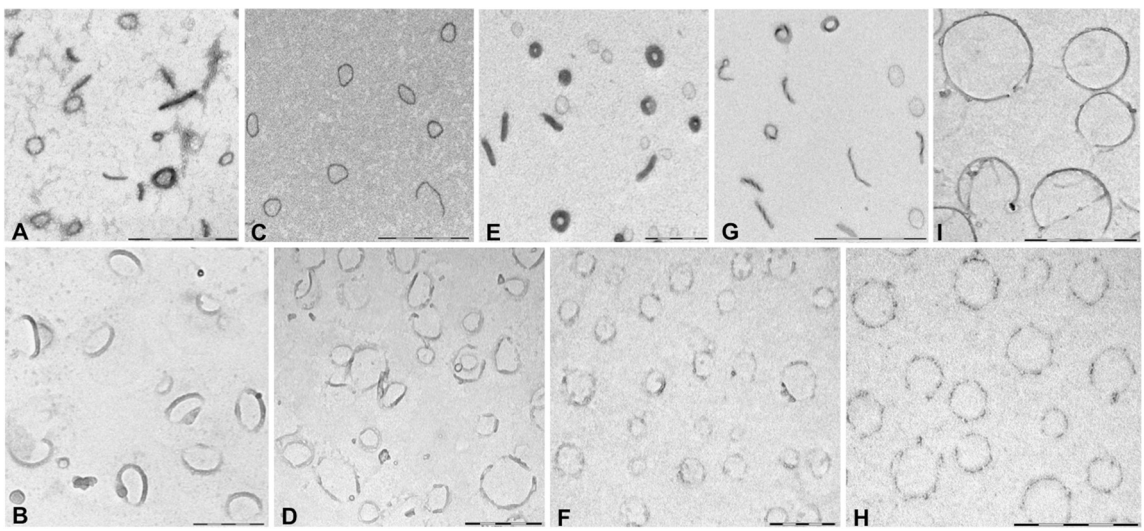

Fig. 3 Upper panel: TEM images of polyplexes (N/P ratio of 20 : 1) placed on a carbon film-coated copper grid and stained with 2% uranyl acetate (A, C, E and G). Lower panel: TEM images of the replica obtained after freeze-fixation and freeze-drying of a 50 mm aqueous solution of polyplexes at a N/P ratio of 20 (B, D, F and H) on an uncoated coverslip. (I) is a replica obtained after freeze-fixation and freeze-drying of free pDNA. Scale bars shown are of either 200 nm (for E, B, F and H) or 500 nm (for A, C, D, G and I). (A) and (B) correspond to B6 polyplex; (C) and (D) to B6mod polyplex; (E) and (F) to c(RGDfK) polyplex; (G) and (H) to Ala polyplex; (I) is free pDNA.

diameter. The upper images in Fig. 3(A), (C), (E) and (G) show dried polyplexes stained with uranyl acetate. Some other of these structures adopted a more "rod-like" shape. In Fig. 3 lower images (B), (D), (F) and (H) the same polyplexes were freeze-dried, keeping the shape and structure as they appear in solution. From these images it can be inferred that the preferred shape of the polyplexes is the "doughnut" shape, a common configuration of several pDNA–polycation polyplexes.[54] Fig. 3I shows a freeze-dried replica of pDNA alone. The rounded shape is much larger (around 350 nm) than that of the polyplexes (70–100 nm), indicating a clear compaction of the pDNA when the polymers are present. However, this compaction was not maximal with the PEG-containing polymers. The analogous polyplexes formed with pDNA and Ala polymer lacking PEG moiety, $(C\text{-}Stp_4)_2$-K-A, showed a more compact shape of around 40 nm (see Fig. S8, ESI†). Presumably and not surprisingly, the high content of PEG (24 monomer units compared to 8 Stp units, *i.e.* 24 protonable ethane amino units) in the targeting polymers interfered with pDNA condensation, resulting in more loose 'spaghetti-type' nanostructures. AFM images are consistent with the results obtained by TEM (Fig. 4). Dried polyplexes at the same N/P ratio on a mica surface showed similar shapes and polyplex sizes as those observed by TEM. Furthermore, DLS was used to determine polyplex size and also zeta potential (see Fig. S7, ESI†). DLS data are well in agreement with TEM and AFM; the apparent high polydispersity index PDI of 0.2–0.5 does not correlate with the observed homogeneity but is consistent with the fact that particles are not fully compacted into solid spheres because of the high PEG content. DLS of uncomplexed polymers without pDNA did not show detectable nanostructures in water for all four ligand–PEG polymers (data not shown), which is in line with their largely hydrophilic character. Polyplexes containing polymer and a PEG moiety in their structure (with the exception of B6 polymer) showed a zeta potential of nearly zero, indicating almost no charge on their surface. The PEG moiety acts as a "charge-shielding moiety", which may prevent non-specific interactions between the polyplex and the negatively charged cell surfaces. In contrast, the zeta potential of polyplexes containing B6 polymer was around +12 to 15 mV at N/P ratios of 6 to 20 (see Fig. S7, ESI†). This finding can be explained by the presence of the positive amino acid residues of the B6 sequence, which might be responsible for some non-specific interactions of B6-polyplexes with cells (see below).

Our structures contained two terminal cysteine residues at the end of each polymeric branch (Fig. 1). The presence of these residues in related peptide-based gene delivery vectors improves pDNA complexation and thus its delivery efficiency.[55–57] This improvement has also been demonstrated in our recent study with Stp-based non-targeted polyplexes[32]. Disulfide bridge formation is thought to be relevant in the stabilization of polyplexes, as these bridges can further increase polyplex compaction by forming a surrounding "cage". Polyplexes would then be stabilized not only by electrostatic interactions but also by the presence of disulfide bridges. Our cysteine-containing polymers showed accelerated disulfide bridge formation in the presence of pDNA (Fig. 5), which is consistent with previously published work on template-assisted oligomerization.[32,58,59] The presence of DNA catalyzed the formation of disulfide bridges, as the local concentration of free thiols was greatly increased as a result of the electrostatic interactions between the negatively charged DNA and the cationic polymer.

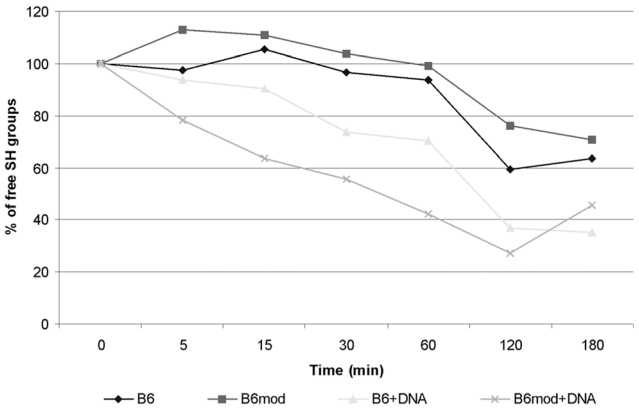

Fig. 5 DNA-template mediated acceleration of disulfide-bridge formation. Detection of free thiol groups over time as an indicator of disulfide formation in the absence or presence of pEGFPLuc DNA ("DNA"). Polymer solutions or corresponding pDNA polyplexes polymer/pDNA ratio of N/P 12 in HBG were incubated at room temperature (RT). At the indicated time points, 10 μL of the solutions were diluted with Ellman's buffer and DNTB stock solution. The samples were then measured at 412 nm. The 100% value represents the concentration of the cysteine mercapto group of the polymer at the starting point.

Transfection efficacy

After studying the biophysical aspects of the polyplexes, we assessed the capacity of these polymers to deliver pDNA into the cells in a receptor-specific way. The high PEG content of the polyplexes should reduce non-specific internalization by shielding positive charges of the polymer backbone from the polyplex surface. Thus unspecific interactions of the polyplex backbone with the negative glycocalix of the cells should be reduced. When the peptide moiety is unsuitable for receptor binding, cell binding and endocytosis should be low. After endocytosis, the polyplex must escape from the endosome and deliver the pDNA to the nucleus where gene expression starts to take place. For the targeting studies, we used mouse neuroblastoma (N2A) and human prostate adenocarcinoma (DU-145) cells. These are tumor cell lines that overexpress both TfR[60,61] (for B6 peptide binding) and integrins[49] (for c(RGDfK) binding).

The transfection efficiency of pDNA polyplexes was tested by a standard luciferase gene transfer assay. A fixed amount of pDNA (200 ng, pCMVeGFPLuc) was complexed with the polymers at the indicated N/P molar ratios. Fig. 6 shows the luciferase gene transfer activity of B6 and B6mod polymers in N2A and DU-145 cells. Polyplexes at various N/P ratios (6, 12 and 20) were incubated with cells for 1 h. The medium was removed afterwards and cells were washed with PBS. When indicated, a concentration of 100 μM of chloroquine was added to the medium in order to enhance the endosomal escape of the polyplexes, as chloroquine is a commonly used endolysosomotropic weak base. By accumulating in endolysosomes and buffering pH, chloroquine triggers osmotic effects that promote an increased release of entrapped drugs or non-viral vectors into the

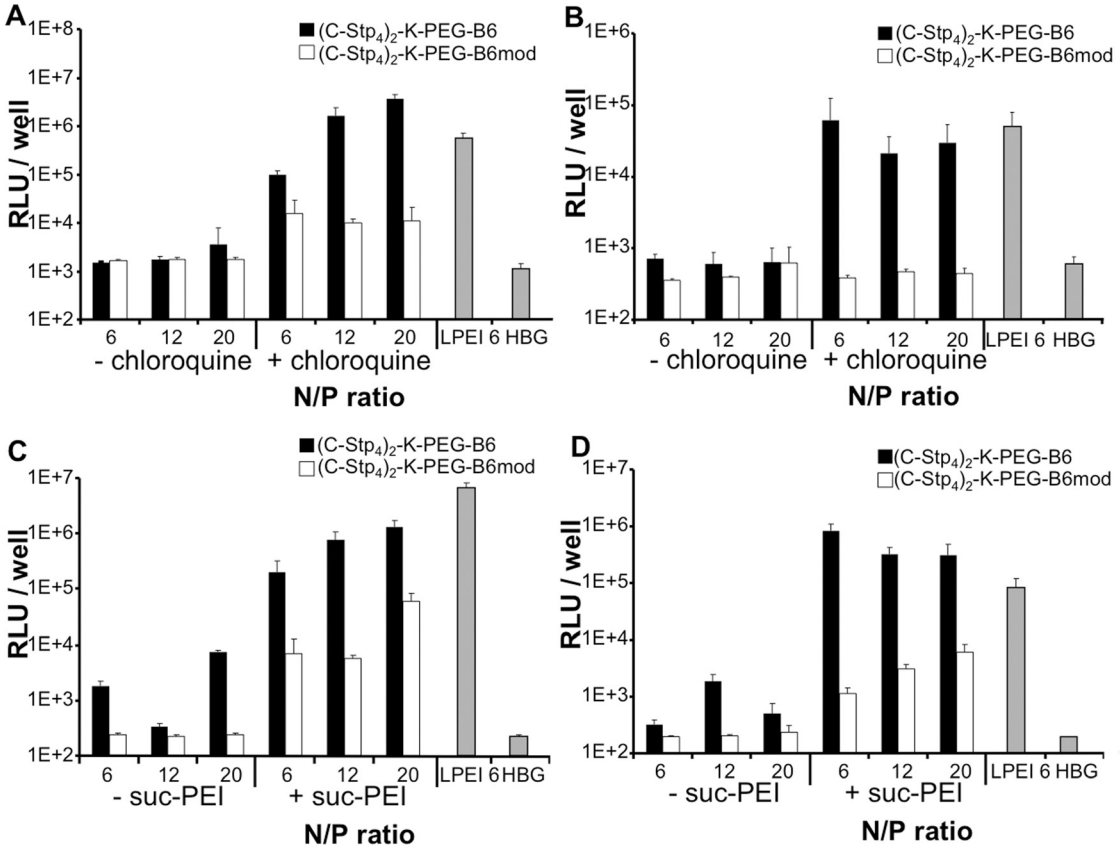

Fig. 6 Transfection of N2A (A, C) and DU-145 (B, D) cells with pDNA-B6 and B6mod polyplexes at 6, 12 and 20 N/P ratios. After a 1 h incubation at 37 °C and 5% CO_2, medium was removed and replaced by fresh one. Where indicated, 100 μM chloroquine was added in (A) and (B) or 0.8 μg suc-PEI/well was added in (C) and (D) as described in Materials and methods. Linear polyethylenimine (LPEI) was used as a positive control and HBG as a negative one.

cytosol.[50,62] The addition of this endosomolytic agent strongly (by >2 log units) enhanced the activity of B6-bearing polyplexes compared with the transfection efficacy of polyplexes carrying the modified version of B6 peptide (Fig. 6A and B). The addition of chloroquine was an essential step for these vectors to be effective, but it also induces significant cytotoxicity (see Fig. S9–S12, ESI†, for the MTT assays). In order to further demonstrate the capacity of the targeting polymers to effectively deliver pDNA to the cells, we chose another recently developed less cytotoxic endosomolytic agent (succinylated polyethylenimine, suc-PEI) to induce polyplex release from the endosomes (Fig. 6C and D). Suc-PEI has endosomal proton buffering capacity but is less toxic than PEI. This agent can also be added to transfections separately from the transfection polyplexes.[63] Consistent with the effect of chloroquine, suc-PEI increased the transfection efficacy of the polyplexes by more than 1000-fold. Once again, the targeting polyplexes were more than 100 times more effective than the controls in the presence of this endosomolytic agent. But remarkably, suc-PEI showed lower toxicity than chloroquine (see Fig. S9–S12, ESI†, for the MTT assays). The optimum gene transfection results were observed at a N/P ratio of 20 in the case of N2A cells and at a N/P ratio of 6 in the case of Du-145 cells. These differences are attributed to the individual characteristics of each cell line, as particle size is not significantly different (see ESI† for DLS data).

We then addressed whether these findings are also relevant for another ligand–receptor pair with potential in tumor targeting. For this purpose we chose the c(RGDfK) peptide as a very specific high-affinity ligand for $\alpha_v\beta_3$ integrins, which are overexpressed in tumor tissue and tumor cells. $\alpha_v\beta_3$ integrin is also overexpressed in N2A and DU-145 cells. Transfection of DU-145 cells with c(RGDfK) or Ala polyplexes at various N/P ratios (Fig. 7A) highlighted the effect of the integrin ligand. In the presence of chloroquine, luciferase expression was enhanced in cells incubated with c(RGDfK), reaching 1400-fold higher expression over the Ala control polyplexes. The transfection efficacy of polyplexes containing the c(RGDfK) peptide was 70 times higher than that of linear PEI (LPEI) polyplexes. The transfection results in N2A cells (Fig. 7B) or DU-145 cells (Fig. 7C) in the presence of suc-PEI gave the same results. The c(RGDfK) polymer achieved up to 1000-fold higher expression levels than the ligand-free PEGylated control polyplex. Again, the toxicity of suc-PEI was found to be lower than that of chloroquine (see Fig. S9–S12, ESI†).

With the aim to further demonstrate the specificity of the binding of these polyplexes to their receptors, we performed receptor blocking experiments. DU-145 cells were treated either with free iron-loaded transferrin or with the super potent integrin antagonist RGD peptide cilengitide[64,65] prior to transfection, in order to block their cell-surface expressed specific receptors

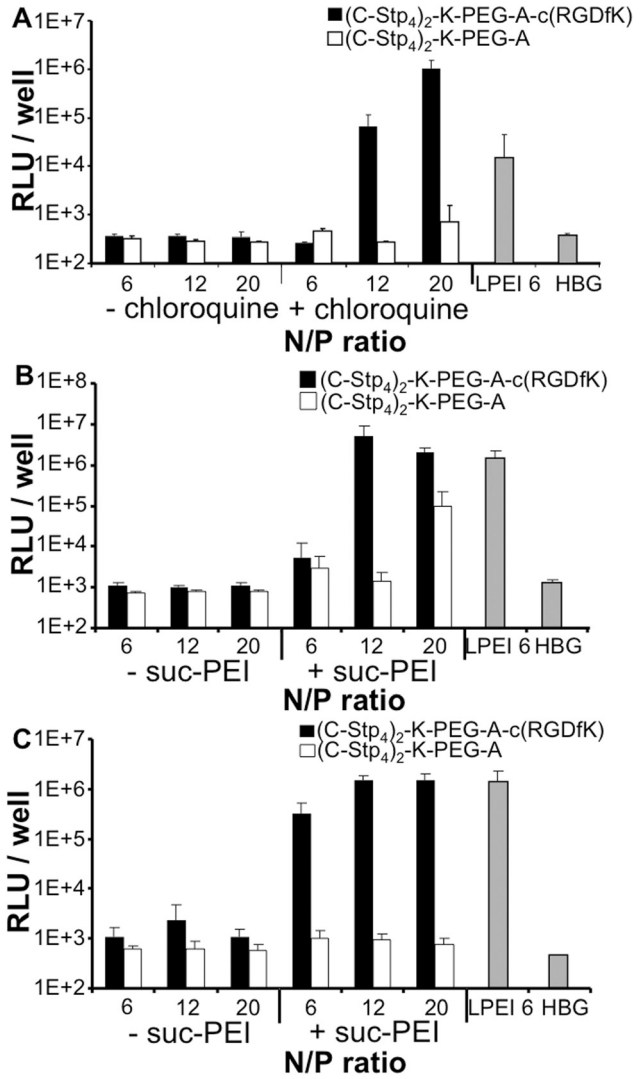

Fig. 7 Transfection of DU-145 (A, C) or N2A (B) cells with c (RGDfK) or Ala polyplexes. After 1 h incubation at 37 °C and 5% CO_2, medium was removed and replaced by fresh one. Where indicated, 100 μM chloroquine was added in (A) or 0.8 μg suc-PEI/well was added in (B, C) as described in Materials and methods. LPEI used as a positive control and HBG as a negative one.

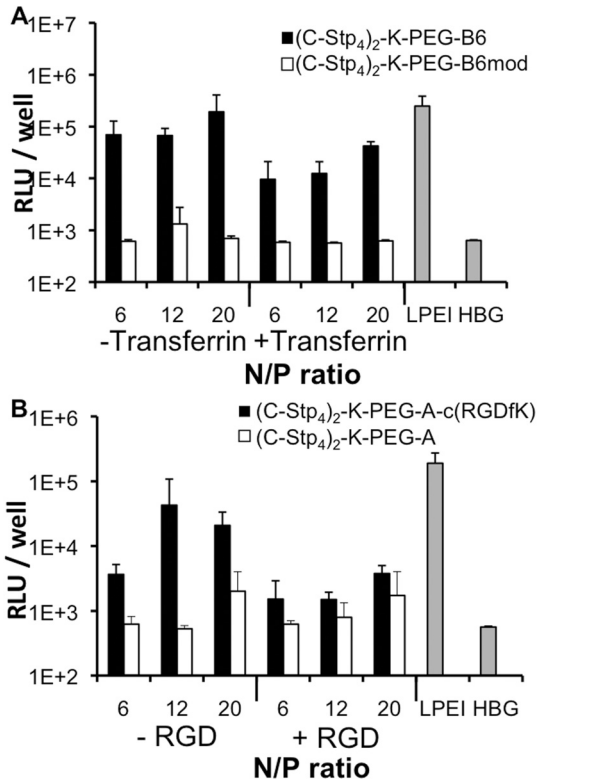

Fig. 8 Receptor blocking assays in DU-145 cells by (A) the soluble transferrin protein (+Transferrin) with B6 polyplexes, and (B) soluble cilengitide (+RGD) with c(RGDfK) polyplexes. Cells were treated where indicated with the free molecules for 10 min at 4 °C to allow binding on the transferrin receptor (TfR) or $\alpha_v\beta_3$. Polyplexes at the indicated N/P ratio were then added to the cells. After 1 h of polyplex incubation at 37 °C and 5% CO_2, medium was removed and replaced by a fresh one. In all the cases 100 μM chloroquine was added, as described in Materials and methods. LPEI was used as a positive control and HBG as a negative one.

(TfR and $\alpha_v\beta_3$ integrin, respectively) and to prevent polyplex internalization, thereby demonstrating the specificity of the constructs. DU-145 cells treated with free transferrin for competitive inhibition of B6 polyplex binding showed a 7-, 6- or 5-fold decrease in the B6 polyplex-mediated transfection levels, at a N/P ratio of 6, 12 and 20, respectively (Fig. 8A). Transferrin competition did not restore expression to the background levels of the B6mod polyplexes, most probably because of the cationic nature of the B6 ligand, which – in contrast to the other PEG-shielded polyplexes – results in a positive zeta potential (see Fig. S7, ESI†) and triggers moderate cell interaction that is not dependent on the TfR. Furthermore, competition experiments using a fixed amount of B6 polyplexes (N/P = 6) and increasing concentrations of free transferrin (0, 20 and 50 mol equivalents) were performed in DU-145 and N2A cells (see Fig. S13, ESI†). When chloroquine was also present, we detected an increasing reduction of luciferase expression with rising amounts of free transferrin (10-fold or 3-fold reduction of the B6 polyplex mediated transfection levels in N2A or DU-145 cells, respectively). Again, background expression levels were not reached due to the positives charges of B6, as expected, but a TfR-competition effect on gene expression was observed in both cell lines.

In the case of the c(RGDfK) polymer, a higher reduction of c (RGDfK)-mediated transfection was observed when cells were first incubated with cilengitide (Fig. 8B). In this case, at a N/P ratio of 12, competitive inhibition of cilengitide resulted in nearly 30-fold decrease in luciferase expression (and 3- or 6-fold reduction for N/P 6 and 20, respectively). Here, cilengitide competition decreased gene expression to almost background levels, thereby indicating very low non-specific cell internalization. The specific character of this internalization was also confirmed by zeta potential measurements for c(RGDfK) polyplex, which revealed that these polyplexes did not carry a surface charge (see Fig. S7, ESI†). Taken together, these results further validate the concept of TfR- and $\alpha_v\beta_3$-targeted gene delivery in the presence of an endosomolytic agent such as chloroquine. Moreover, cilengitide competition experiments using LPEI showed no

competitive effect, in contrast with observations in c(RGDfK) polyplex transfection (Fig. S14, ESI†).

The positive ligand effect observed on polyplex transfection is very encouraging for the further development of defined polymers based on oligo(ethane amino)amide building blocks. However, all these data show that the polyplexes tested are strictly dependent on help by endosomolytic agents. This observation is not surprising as endosomal release is one of the major bottlenecks in the intracellular delivery field.[66] Erythrocyte lysis assays did not show any detectable lytic activity of the polymers at any pH (see Fig. S15, ESI†). The current Stp polymers, however, do contain protonable ethane amino units similar to PEI. Non-targeted, non-PEGylated Stp-based polymers have been shown to mediate high gene transfer activity in the absence of endosomal release agents.[32] In contrast, the new-targeted polymers presented in the current study have a very high PEG content (equal numbers of protonable ethylenimine units as ethylene glycol units). This feature has not only been shown to shield polyplexes but also to inactivate endosomal release of PEI-based polyplexes.[26] Therefore other methods should be considered to promote endosomal escape, by either enhancing the proton sponge effect of the targeting polymer or introducing another endosomolytic function into the polymer such as acid labile groups between PEG and carrier polymer[26,27] or endosomolytic peptides.[6,10,11] Nevertheless, our current results show the feasibility of designing newly defined, non-toxic polymers for receptor-targeted gene delivery.

Conclusions

Here we designed two fully synthetic polymers for receptor-targeted pDNA transfection. Solid-phase supported synthesis using novel building blocks provided full control of the sequence and composition of each polymer. This approach enabled the generation of precise multidomain polymers containing the following: (i) a peptidic targeting ligand; (ii) a precise PEG shielding molecule; (iii) oligo(ethane amino)amides for pDNA binding; and (iv) terminal cysteine residues for disulfide bridge-driven stabilization. Peptide ligands targeting the TfR or $\alpha_v\beta_3$ integrins were examined. Targeting polymers in combination with endosomolytic agents mediated strongly ligand-dependent gene transfer in receptor-overexpressing tumor cells. Efforts devoted to the further development of this targeted and shielded precise carrier are now centered on the bottleneck of endosomal escape, which continues to be a major challenge in the field of intracellular gene delivery.

Materials and methods

Materials

Fmoc-*N*α-protected amino acids were obtained from IRIS Biotech GmbH (Marktredwitz, Germany). Fmoc-*N*-amido-dPEG®$_{24}$-acid was obtained from Quanta Biodesign (Ohio, USA); Stp units were synthesized as described before.[31] The 2-chlorotrityl chloride resin was purchased from IRIS Biotech GmbH (Marktredwitz, Germany). Coupling reagents: benzotriazol-1-yloxytris(pyrrolidino)phosphonium hexafluorophosphate (PyBOP) was from Novabiochem (Laüfelfingen, Switzerland); 1-hydroxy-7-azabenzotriazole (HOAt) was from GL Biochem (Shanghai, China); 2-(1*H*-benzotriazol-1-yl)-1,1,3,3-tetramethyluronium tetrafluoroborate (TBTU) was from Albatros Chem, Inc. (Montreal, Canada); (2-(7-aza-1*H*-benzotriazole-1-yl)-1,1,3,3-tetramethyluronium hexafluorophosphate) (HATU) was from Medalchemy (Alicante, Spain). Trifluoroacetic acid (TFA) was purchased from Scharlab S.L. (Barcelona, Spain); piperidine from SDS (Peypin, France), dimethylformamide (DMF) from IRIS Biotech GmbH (Marktredwitz, Germany) and dichloromethane (DCM) and acetonitrile (MeCN) from Sigma (St. Louis, MO). *N*,*N*-Diisopropylethylamine (DIEA) was obtained from Merck (Darmstadt, Germany) and hexafluoroisopropanol (HFIP) from Sigma (St. Louis, MO). Triisopropylsilane (TIS) was from Fluka (Buchs, Switzerland). Heparin sodium salt from porcine intestinal mucosa (MW = 17–19 kDa) was from Sigma (St. Louis, MO); GelRed was obtained from Biotium (Hayward, USA); 5,5′-dithio-bis(2-nitrobenzoic acid) (DTNB) was from Merck (Darmstadt, Germany) and agarose was supplied by Invitrogen (Darmstadt, Germany).

Polymer synthesis

B6- (peptide sequence: GHKAKGPRK), B6mod- (peptide sequence: GHGAGGPGG), and Ala (C-Stp$_4$)$_2$-K-PEG polymers were synthesized following standard SPPS procedures using an orthogonal Fmoc/*t*Bu strategy and L-amino acids. A precise bifunctional Fmoc-*N*-amido-dPEG®24-acid and the novel Boc/Fmoc artificial oligoamino acid building blocks (succinoyl tetraethylene pentamine (Stp)[31]) were introduced under the same conditions. The solid support was 2-chlorotrityl chloride resin in a scale between 20 and 150 μmol using a 2 mL or 5 mL syringe reactor (Multisynthec GmbH, Witten, Germany), each fitted with a polyethylene porous disk. Solid-phase peptide elongation and other solid-phase manipulations were carried out at room temperature (RT), and solvents and soluble reagents were removed by suction. Washing procedures between synthesis steps were performed with DMF (5 × 30 s) and DCM (5 × 30 s) using 5 mL solvent per gram of resin. During couplings the mixture was allowed to react with intermittent manual stirring. For the c(RGDfK) polymer, the peptide and the polymeric body were synthesized separately in a fully protected form and coupled afterwards in solution. The protected cyclic peptide c(-Arg(Pbf)-Gly-Asp(O*t*Bu)-D-Phe-Lys-) was synthesized manually in solid-phase following previously described methods.[34,35] For the synthesis of the polymer–c(RGDfK) conjugate, the protected polymeric scaffold ([Cys(Trt)-(Stp(Boc$_3$))$_4$]$_2$-Lys-PEG-Ala) (1.1 equiv.), HATU (1.2 equiv.) and HOAt (1.2 equiv.) were dissolved in anhydrous DMF to reach a concentration of 0.02 mM. After the addition of DIEA (5 equiv.), the mixture was pre-activated for 4 h. Next, c(-Arg(Pbf)-Gly-Asp(O*t*Bu)-D-Phe-Lys-) (1 equiv.) dissolved in the minimum volume of anhydrous DMF was added to the reaction mixture dropwise and the solution was stirred for one week at RT. After this time, DMF was evaporated to dryness, and a saturated solution of $NaHCO_3$ was added to the crude product, which was then extracted three times with EtOAc. The organic phase was washed with brine and dried with Na_2SO_4. After evaporation, the polymer–c(RGDfK) conjugate was obtained free of coupling reagents. To remove side chain

protecting groups, the polymer construct was treated for 3 h with TFA–H_2O–TIS (95 : 2.5 : 2.5, v/v/v) at RT. Next, the compound was precipitated with cold anhydrous Et_2O, centrifuged for 10 min at 4000 rpm, washed twice with this solvent and finally redissolved in water and lyophilized.

Initial conditioning of resin. 2-Chlorotrityl chloride resin was used in all cases and conditioned by swelling in DCM (15 min). The first Fmoc-amino acid (0.7 equiv.) was then attached to the resin with DIEA (7 equiv.) in DCM (2 mL) for 1 h, without filtration. The remaining active positions were capped by methanol (0.8 mL g^{-1} of resin) for 15 min. The resin was filtered and washed with DCM (5 × 30 s). The Fmoc group was removed, and filtrates were collected and measured by UV spectroscopy to determine the loading capacity (0.6 mmol g^{-1}).

Fmoc group removal. To remove the Fmoc group, we treated the resin with piperidine in DMF (1 : 4 (v/v), 3–4 mL g^{-1} resin, 1 × 1 min and 2 × 10 min).

Elongation. Couplings of polyamine building blocks (Stp), defined PEG or amino acids were done by dissolving 4 equiv. of the Fmoc-protected version of them, PyBOP–HOBt (4 equiv.), DIEA (8 equiv.) in the minimal amount of DMF–DCM. After 45 min of incubation in the syringe reactor, the completeness of the coupling reaction was checked by the Kaiser test.[67]

Cleavage of polymers. For the cleavage of all the structures (with the exception of the c(RGDfK)–polymer), the dry resin was treated with a TFA–H_2O–TIS (95 : 2.5 : 2.5, v/v/v) mixture for 1 h (10 mL g^{-1} resin). The resin was filtered and washed twice with DCM. After polymer cleavage, the solvent was evaporated. The product was precipitated in ice-cold *t*BME and the precipitate was isolated by centrifugation. The pellet was dissolved in H_2O–MeCN (1 : 1) and freeze-dried. Cleavage of the c(RGDfK) polymeric scaffold ([Cys(trt)-Stp(Boc_3)$_4$]$_2$-Lys–PEG–Ala) from the resin was performed fully protected by incubating the resin 5 times for 5 min with 10% HFIP in DCM. DCM was subsequently evaporated.

The polymers were identified at λ = 220 nm by analytical RP-HPLC (Waters 2998 photodiode array detector equipped with the Waters 2695 separation module, Sunfire C4 column (150 × 4.6 mm, 5 μm, 100 Å, Waters), and the Millenium software; flow rate = 1 mL min^{-1}; gradient = 0–100% B in 15 min; A = 0.045% TFA in H_2O, B = 0.036% TFA in MeCN), ^{1}H-NMR and high resolution mass spectra (LTQ-FT Ultra (Thermo Scientific)).

Proton NMR spectra. ^{1}H-NMR spectra were recorded using a JNMR-GX 400 (400 MHz) or JNMR-GX 500 (500 MHz) unit produced by Jeol. All spectra were recorded without tetramethylsilane (TMS) as internal standard and therefore all signals were calibrated to the residual proton signal of the solvent. The coupling constant had an accuracy of 0.3 Hz.

DNA polyplex formation. Polyplex formulations for transfection and gel shift experiments were prepared as follows: 200 ng of pDNA and the calculated amount of polymer were diluted in separate tubes each in 10 μL of 20 mM HEPES buffer with 5% glucose pH 7.4 (HBG). The polycation solution was added to the nucleic acid, rapidly mixed by pipetting up and down (at least 5 times) and incubated for 30 min at RT in order to form the polyplexes.

Transmission electron microscopy. Freeze-drying: Drops (50 μL) of aqueous solutions of the polyplexes (200 μg pDNA and polymer in a N/P ratio of 20) or free pDNA (20 μg μL^{-1}) were deposited on uncoated cover slips. These were then freeze-fixed by projection against a copper Cryoblock cooled by liquid nitrogen (−196 °C) (Reichert-Jung, Leica, Germany). The frozen samples were stored at −196 °C in liquid nitrogen until subsequent use. Samples were freeze-dried at −90 °C and coated with platinum and carbon by using a freeze-etching unit (model BAF-060, BALTEC, Liechtenstein). Rotatory shadowing of the exposed surface was performed by evaporating 1 nm of platinum–carbon at 6 °C above the horizontal plane, followed by 10 nm of carbon evaporated at 90 °C. The replica was separated from the cover slip by immersion in concentrated hydrofluoric acid, and was washed twice with distilled water and digested with sodium hypochlorite (5%, v/v) for 5 to 10 min. The replicas were washed several times in distilled water and collected on Formvar-coated copper grids for electron microscopy. Negative dye: Drops (50 μm) of aqueous solutions of the polyplexes (200 μg pDNA and polymer in N/P ratio of 20) or free pDNA (20 μg μL^{-1}) were deposited on carbon film-coated copper grids for 1 min. After that, grids were washed (2 × 1 min) with water and finally stained with 2% uranyl acetate (1 min). When the grids were dry, electron micrographs were obtained. All micrographs were obtained by using a Jeol JEM 1010 MT electron microscope (Japan) operating at 80 kV. Images were obtained on a CCD camera Megaview III (ISIS, Münster, Germany). The results obtained by TEM imaging were found to be reproducible within >50 (independent) measurements.

Atomic force microscopy (AFM). AFM imaging was performed with a commercial multimode atomic force microscope controlled by Nanoscope IV electronics (Digital Instruments). 10 μL of the sample were allowed to adsorb for 5–10 min at RT on a freshly cleaved, highly ordered mica surface and finally imaged in tapping mode operation.

DNA binding assay. A 1% agarose gel was prepared by dissolving agarose in TBE buffer (trizma base 10.8 g, boric acid 5.5 g, disodium EDTA 0.75 g, and 1 L of H_2O) and boiling to 100 °C. After cooling to about 50 °C and addition of GelRed, the agarose gel was cast in the electrophoresis unit. Polyplexes, containing 200 ng of pDNA in 20 μL HBG and loading buffer (prepared from 6 mL of glycerin, 1.2 mL of 0.5 M EDTA, 2.8 mL of H_2O, 0.02 g of bromophenol blue) were placed into the sample pockets. Electrophoresis was performed at 80 V for 80 min.

Measurement of particle size and zeta potential *via* dynamic light scattering (DLS). Particle size of pDNA formulations and zeta potentials were measured by laser-light scattering using a Zetasizer Nano ZS (Malvern Instruments, Worcestershire, U.K.). pDNA polyplexes with 10 μg pEGFPLuc were prepared in 1 mL 20 mM HEPES (4-(2-hydroxyethyl)-1-piperazineethanesulfonic acid) buffer pH 7.4 and measured after 30 min of incubation.

Ellman's assay.[68] 0.4 mg of DTNB dissolved in 1 mL of the corresponding Ellman's buffer (0.2 M Na_2HPO_4 with 1 mM

EDTA at pH 8.0) was used as stock solution. For UV/VIS absorption measurement Ellman's stock diluted 1 : 10 in Ellman's buffer was taken as blank. Samples were diluted in Ellman's buffer and 10% (v/v) of the stock solution. After 15 min at 37 °C the solutions were measured at 412 nm. Concentrations of the free thiols at 0 min were set to 100%. For the determination of free thiol groups over time, the polymer or polyplex samples were processed as described above.

Cell culture. Mouse neuroblastoma cells (N2A) and human prostate adenocarcinoma cells (DU-145) were obtained from American Type Culture Collection ATCC (Rockville, MD, USA). N2A were grown in Dulbecco's modified Eagle's medium (DMEM) 4500 mg glucose L^{-1}, supplemented with 10% FCS, 4 mM stable glutamine, 100 U mL^{-1} penicillin, and 100 μg mL^{-1} streptomycin. DU-145 cells were grown in RPMI-1640 medium supplemented with 10% fetal calf serum (FCS), 4 mM stable glutamine, 100 U mL^{-1} penicillin, and 100 μg mL^{-1} streptomycin. Exponentially growing cells were detached from the culture flasks by using a trypsin–EDTA (0.25%) solution and the cell suspension was seeded at the required concentration for each experiment.

Gene transfer. Cells were seeded 24 h prior to pDNA delivery using 10 000 cells per well in 96-well plates. Transfection efficiency of the polymers was evaluated using 200 ng pEGFPLuc DNA per well. All experiments were performed in quintuplicate. At day of transfection medium was replaced with 80 μL fresh medium containing 10% FCS. Transfection complexes formed at various protonable nitrogen/phosphate (N/P) ratios in 20 μL HBG were added to each well and incubated at 37 °C. After 1 h of incubation, the medium was removed and the cells washed twice with phosphate-buffered saline (PBS). 90 μL of fresh medium and 100 μM chloroquine in 10 μL PBS, 0.8 μg suc-PEI in 10 μL PBS or 10 μL of PBS were added. In the case of DU-145 cells, medium was removed again after 4 h and replaced by fresh one. For the positive control, 0.8 μg of linear PEI was mixed with pDNA (see pDNA polyplex formation section) and polyplexes were treated the same way as all the others. As negative control, cells were treated with 20 μL HBG buffer. 24 h after transfection, cells were treated with 100 μL cell lysis buffer (25 mM Tris, pH 7.8, 2 mM EDTA, 2 mM DTT, 10% glycerol, 1% Triton X-100). Luciferase activity in the cell lysate was measured using a luciferase assay kit (100 μL Luciferase Assay buffer, Promega, Mannheim, Germany) and a Lumat LB9507 luminometer (Berthold, Bad Wildbad, Germany).

Transferrin and cilengitide competition assay. DU-145 cells were seeded 24 h prior to pDNA delivery using 10×10^4 cells per well in 96-well plates. Transfection efficiency of the polymers in the presence or absence of transferrin (Tf) and cilengitide was evaluated using 100 ng pEGFPLuc DNA per well. All experiments were performed in quintuplicate. On the day of transfection medium was replaced with 90 μL fresh medium containing 10% FCS. The competing cells were incubated with 226 μg/well of iron-loaded (Fe-citrate, 1.25 μg mg^{-1} Tf) Tf (human Tf from Sigma) or with 0.84 μg/well of cilengitide in 90 μL medium for 10 min at 4 °C in order to allow Tf and cilengitide to bind to their corresponding receptors but preventing from their internalization. Afterwards, transfection complexes formed at N/P ratios of 6, 12 and 20 in 10 μL HBG were added to each well and incubated at 37 °C. After 1 h of incubation, the medium was removed and 100 μL of fresh medium containing 100 μM chloroquine were added. Medium was removed again after 4 h and replaced by a fresh one. For the positive control, 0.8 μg of linear PEI was mixed with pDNA and polyplexes were treated the same way as all the others. As negative control, cells were treated with 10 μL HBG buffer. 24 h after transfection, cells were treated with 100 μL cell lysis buffer (25 mM Tris, pH 7.8, 2 mM EDTA, 2 mM DTT, 10% glycerol, 1% Triton X-100). Luciferase activity in the cell lysate was measured using the luciferase assay kit. For the competition assay with increasing concentrations of Tf, the same protocol was followed with slight modifications. DU-145 and N2A cells were seeded 24 h prior to pDNA delivery using 10 000 cells per well in 96-well plates. Transfection efficiency of the polymers in the presence or absence of Tf was evaluated using 200 ng pEGFPLuc DNA per well. At day of transfection medium was replaced with 80 μL fresh medium containing 10% FCS. The cells were incubated with no Tf, 90 or 226 μg iron-loaded Tf/well for 30 min at 4 °C. Afterwards B6 transfection complexes formed at N/P ratio of 6 in 20 μL HBG were added to each well and incubated for 1 h at 37 °C. The medium was then removed and the cells washed twice with PBS. 90 μL of fresh medium and 100 μM chloroquine in 10 μL PBS or 10 μL of PBS were added. Medium was removed again after 4 h and replaced by a fresh one. For the positive control, 0.8 μg of linear PEI was mixed with pDNA and polyplexes were treated the same way as the experiment described above. As negative control cells were treated with 20 μL HBG buffer. 24 h after transfection the luciferase expression was measured as described before.

Cytotoxicity assay of polyplexes. N2A and DU-145 cells were seeded into 96-well plates at a density of 1×10^4 cells/well. After 24 h, culture medium was replaced with 80 μL fresh growth medium containing 10% FCS and transfection complexes (20 μL in HBG) at various N/P ratios were added. When chloroquine or suc-PEI was needed, it was added following the same protocol used for the transfection experiments. All studies were performed in quintuplicate. 22 h post transfection, 10 μl MTT (5 mg mL^{-1}) were added to each well reaching a final concentration of 0.5 mg MTT/mL. After an incubation time of 2 h, unreacted dye and medium were removed. For cell lysis, samples were frozen at −80 °C for 2 h. The purple formazan product was dissolved in 100 μL/well dimethyl sulfoxide (DMSO) and quantified by a microplate reader (Spectrafluor Plus, Tecan Austria GmbH, Grödig, Austria) at 590 nm with background correction at 630 nm. The relative cell viability (%) compared to control cells containing cells treated with HBG was calculated by [A] test/[A]control × 100.

Erythrocyte leakage assay. Murine erythrocytes were isolated from fresh citrate-buffered blood and washed with PBS several times. The erythrocyte pellet was diluted to 5×10^7 erythrocytes per mL with PBS (pH 7.4, 6.5 and 5.5). Polymers were serially diluted in 75 μL of PBS at concentrations of 7.5, 5 and 2.5 μM, respectively, using a V-bottom 96-well plate (NUNC, Denmark). For 100% lysis, control wells contained buffer with 1% Triton

X-100. A volume of 75 μL of erythrocyte suspension was added to each well, and the plates were incubated at 37 °C under constant shaking for 1 h. After centrifugation 80 μL of the supernatant was analyzed for hemoglobin release at 405 nm using a microplate plate reader (Spectrafluor Plus, Tecan Austria GmbH, Grödig, Austria).

Acknowledgements

We thank Olga Brück (LMU Munich) for skilful assistance. This work was supported by the DFG excellence cluster Nanosystems Initiative Munich (NIM), a grant by Roche Kulmbach, and the Munich Biotech Cluster m4 T12. We thank Dr Marta Vilaseca from the Mass Spectrometry Core Facility, IRB Barcelona, for high-resolution mass spectral analyses. This work was also supported by the Ministerio de Educación y Ciencia (FPU), and by the European Molecular Biology Organization through providing a short-term fellowship for I. Martin as visiting PhD student at LMU Munich.

References

1 S. D. Li, S. Chono and L. Huang, *Mol. Ther.*, 2008, **16**, 942–946.
2 V. Russ and E. Wagner, *Pharm. Res.*, 2007, **24**, 1047–1057.
3 M. E. Davis, J. E. Zuckerman, C. H. J. Choi, D. Seligson, A. Tolcher, C. A. Alabi, Y. Yen, J. D. Heidel and A. Ribas, *Nature*, 2010, **464**, 1067–1070.
4 D. Schaffert, M. Kiss, W. Rödl, A. Shir, A. Levitzki, M. Ogris and E. Wagner, *Pharm. Res.*, 2011, **28**, 731–741.
5 D. W. Pack, A. S. Hoffman, S. Pun and P. S. Stayton, *Nat. Rev. Drug Discovery*, 2005, **4**, 581–593.
6 E. Wagner, *Pharm. Res.*, 2008, **25**, 2920–2923.
7 D. Edinger and E. Wagner, *Wiley Interdiscip. Rev.: Nanomed. Nanobiotechnol.*, 2011, **3**, 33–46.
8 G. Y. Wu and C. H. Wu, *J. Biol. Chem.*, 1987, **262**, 4429–4432.
9 P. L. Felgner, Y. Barenholz, J. P. Behr, S. H. Cheng, P. Cullis, L. Huang, J. A. Jessee, L. Seymour, F. Szoka, A. R. Thierry, E. Wagner and G. Wu, *Hum. Gene Ther.*, 1997, **8**, 511–512.
10 E. Wagner, C. Plank, K. Zatloukal, M. Cotten and M. L. Birnstiel, *Proc. Natl. Acad. Sci. U. S. A.*, 1992, **89**, 7934–7938.
11 M. Meyer, A. Philipp, R. Oskuee, C. Schmidt and E. Wagner, *J. Am. Chem. Soc.*, 2008, **130**, 3272–3273.
12 O. Boussif, F. Lezoualc'h, M. A. Zanta, M. D. Mergny, D. Scherman, B. Demeneix and J. P. Behr, *Proc. Natl. Acad. Sci. U. S. A.*, 1995, **92**, 7297–7301.
13 A. Kichler, C. Leborgne, E. Coeytaux and O. Danos, *J. Gene Med.*, 2001, **3**, 135–144.
14 J. P. Behr, *CHIMIA Int. J. Chem.*, 1997, **51**, 34–36.
15 N. D. Sonawane, F. C. Szoka and A. S. Verkman, *J. Biol. Chem.*, 2003, **278**, 44826–44831.
16 A. Akinc, M. Thomas, A. M. Klibanov and R. Langer, *J. Gene Med.*, 2005, **7**, 657–663.
17 S. M. Moghimi, P. Symonds, J. C. Murray, A. C. Hunter, G. Debska and A. Szewczyk, *Mol. Ther.*, 2005, **11**, 990–995.
18 G. Grandinetti, N. P. Ingle and T. M. Reineke, *Mol. Pharmaceutics*, 2011, **8**, 1709–1719.
19 P. Chollet, M. C. Favrot, A. Hurbin and J.-L. Coll, *J. Gene Med.*, 2002, **4**, 84–91.
20 C. Plank, K. Mechtler, F. C. Szoka and E. Wagner, *Hum. Gene Ther.*, 1996, **7**, 1437–1446.
21 M. Breunig, U. Lungwitz, R. Liebl and A. Goepferich, *Proc. Natl. Acad. Sci. U. S. A.*, 2007, **104**, 14454–14459.
22 C. Lin, C.-J. Blaauboer, M. M. Timoneda, M. C. Lok, M. van Steenbergen, W. E. Hennink, Z. Zhong, J. Feijen and J. F. J. Engbersen, *J. Controlled Release*, 2008, **126**, 166–174.
23 V. Russ, T. Fröhlich, Y. Li, A. Halama, M. Ogris and E. Wagner, *J. Gene Med.*, 2010, **12**, 180–193.
24 M. Kursa, G. F. Walker, V. Roessler, M. Ogris, W. Roedl, R. Kircheis and E. Wagner, *Bioconjugate Chem.*, 2002, **14**, 222–231.
25 O. M. Merkel, O. Germershaus, C. K. Wada, P. J. Tarcha, T. Merdan and T. Kissel, *Bioconjugate Chem.*, 2009, **20**, 1270–1280.
26 G. F. Walker, C. Fella, J. Pelisek, J. Fahrmeir, S. Boeckle, M. Ogris and E. Wagner, *Mol. Ther.*, 2005, **11**, 418–425.
27 C. Fella, G. F. Walker, M. Ogris and E. Wagner, *Eur. J. Pharm. Sci.*, 2008, **34**, 309–320.
28 L. Hartmann, S. Häfele, R. Peschka-Süss, M. Antonietti and H. G. Börner, *Chem.–Eur. J.*, 2008, **14**, 2025–2033.
29 L. Hartmann, *Macromol. Chem. Phys.*, 2011, **212**, 8–13.
30 S. Mosca, F. Wojcik and L. Hartmann, *Macromol. Rapid Commun.*, 2011, **32**, 197–202.
31 D. Schaffert, N. Badgujar and E. Wagner, *Org. Lett.*, 2011, **13**, 1586–1589.
32 D. Schaffert, C. Troiber, E. E. Salcher, T. Fröhlich, I. Martin, N. Badgujar, C. Dohmen, D. Edinger, R. Kläger, G. Maiwald, K. Farkasova, S. Seeber, K. Jahn-Hofmann, P. Hadwiger and E. Wagner, *Angew. Chem., Int. Ed.*, 2011, **50**, 8986–8989.
33 H. Xia, B. Anderson, Q. Mao and B. L. Davidson, *J. Virol.*, 2000, **74**, 11359–11366.
34 R. Haubner, R. Gratias, B. Diefenbach, S. L. Goodman, A. Jonczyk and H. Kessler, *J. Am. Chem. Soc.*, 1996, **118**, 7461–7472.
35 M. Kantlehner, P. Schaffner, D. Finsinger, J. Meyer, A. Jonczyk, B. Diefenbach, B. Nies, G. Hölzemann, S. L. Goodman and H. Kessler, *ChemBioChem*, 2000, **1**, 107–114.
36 M. Aumailley, M. Gurrath, G. Müller, J. Calvete, R. Timpl and H. Kessler, *FEBS Lett.*, 1991, **291**, 50–54.
37 D. Cox, M. Brennan and N. Moran, *Nat. Rev. Drug Discovery*, 2010, **9**, 804–820.
38 T. Arndt, U. Arndt, U. Reuning and H. Kessler, in *Cancer Therapy: Molecular Targets in Tumor Host Interactions*, ed. H. Bioscience, Norfolk, United Kingdom, 2005, pp. 93–141.
39 J. S. Desgrosellier and D. A. Cheresh, *Nat. Rev. Cancer*, 2010, **10**, 9–22.
40 E. Ruoslahti and M. D. Pierschbacher, *Science*, 1987, **238**, 491–497.
41 A. Meyer, J. Auernheimer, A. Modlinger and H. Kessler, *Curr. Pharm. Des.*, 2006, **12**, 2723–2747.
42 B. Felding-Habermann and D. A. Cheresh, *Curr. Opin. Cell Biol.*, 1993, **5**, 864–868.
43 M. Pfaff, K. Tangemann, B. Müler, M. Gurrath, G. Müller, H. Kessler, R. Timpl and J. Engel, *J. Biol. Chem.*, 1994, **269**, 20233–20238.
44 R. P. Harbottle, R. G. Cooper, S. L. Hart, A. Ladhoff, T. McKay, A. M. Knight, E. Wagner, A. D. Miller and C. Coutelle, *Hum. Gene Ther.*, 1998, **9**, 1037–1047.
45 P. Erbacher, J. S. Remy and J. P. Behr, *Gene Ther.*, 1999, **6**, 138–145.
46 R. M. Schiffelers, A. Ansari, J. Xu, Q. Zhou, Q. Tang, G. Storm, G. Molema, P. Y. Lu, P. V. Scaria and M. C. Woodle, *Nucleic Acids Res.*, 2004, **32**, 149.
47 W. J. Kim, J. W. Yockman, J. H. Jeong, L. V. Christensen, M. Lee, Y.-H. Kim and S. W. Kim, *J. Controlled Release*, 2006, **114**, 381–388.
48 M. Oba, S. Fukushima, N. Kanayama, K. Aoyagi, N. Nishiyama, H. Koyama and K. Kataoka, *Bioconjugate Chem.*, 2007, **18**, 1415–1423.
49 Y. Nie, D. Schaffert, W. Rödl, M. Ogris, E. Wagner and M. Günther, *J. Controlled Release*, 2011, **152**, 127–134.
50 M. Cotten, F. Längle-Rouault, H. Kirlappos, E. Wagner, K. Mechtler, M. Zenke, H. Beug and M. L. Birnstiel, *Proc. Natl. Acad. Sci. U. S. A.*, 1990, **87**, 4033–4037.
51 E. Wagner, M. Zenke, M. Cotten, H. Beug and M. L. Birnstiel, *Proc. Natl. Acad. Sci. U. S. A.*, 1990, **87**, 3410–3414.
52 L. Xu, K. F. Pirollo, W. H. Tang, A. Rait and E. H. Chang, *Hum. Gene Ther.*, 1999, **10**, 2941–2952.
53 M. E. Davis, J. E. Zuckerman, C. H. Choi, D. Seligson, A. Tolcher, C. A. Alabi, Y. Yen, J. D. Heidel and A. Ribas, *Nature*, 2010, **464**, 1067–1070.
54 E. Wagner, M. Cotten, R. Foisner and M. L. Birnstiel, *Proc. Natl. Acad. Sci. U. S. A.*, 1991, **88**, 4255–4259.
55 D. Oupicky, A. L. Parker and L. W. Seymour, *J. Am. Chem. Soc.*, 2001, **124**, 8–9.
56 D. L. McKenzie, E. Smiley, K. Y. Kwok and K. G. Rice, *Bioconjugate Chem.*, 2000, **11**, 901–909.
57 C. R. Drake, A. Aissaoui, O. Argyros, J. M. Serginson, B. D. Monnery, M. Thanou, J. H. G. Steinke and A. D. Miller, *Mol. Pharmaceutics*, 2010, **7**, 2040–2055.
58 V. S. Trubetskoy, L. J. Hanson, P. M. Slattum, J. E. Hagstrom, V. G. Budker and J. A. Wolff, *Nucleic Acids Res.*, 1998, **26**, 4178–4185.

59 T. Blessing, J.-S. Remy and J. P. Behr, *J. Am. Chem. Soc.*, 1998, **120**, 8519–8520.
60 K. Reis, J. Hälldin, S. Fernaeus, C. Pettersson and T. Land, *J. Neurosci. Res.*, 2006, **84**, 1047–1052.
61 K. J., H. N. Keer, J. M. Kozlowski, Y. C. Tsai, C. Lee, R. N. McEwan and J. T. Grayhack, *J. Urol.*, 1990, **143**, 381–385.
62 H. Luthman and G. Magnusson, *Nucleic Acids Res.*, 1983, **11**, 1295–1308.
63 A. Zintchenko, A. Philipp, A. Dehshahri and E. Wagner, *Bioconjugate Chem.*, 2008, **19**, 1448–1455.
64 M. A. Dechantsreiter, E. Planker, B. Mathä, E. Lohof, G. N. Hölzemann, A. Jonczyk, S. L. Goodman and H. Kessler, *J. Med. Chem.*, 1999, **42**, 3033–3040.
65 C. Mas-Moruno, F. Rechenmacher and H. Kessler, *Anti-Cancer Drugs*, 2010, **10**, 753–768.
66 A. K. Varkouhi, M. Scholte, G. Storm and H. J. Haisma, *J. Controlled Release*, 2011, **151**, 220–228.
67 A. Madder, N. Farcy, N. G. C. Hosten, H. De Muynck, P. J. De Clercq, J. Barry and A. P. Davis, *Eur. J. Org. Chem.*, 1999, 2787–2791.
68 G. L. Ellman, *Arch. Biochem. Biophys.*, 1959, **82**, 70–77.

